# A Closed-form Energy Model for Multi-Rotors Based on the Dynamic of the Movement

João L. Marins*, Tauã M. Cabreira* and Paulo Ferreira*
*Universidade Federal de Pelotas (UFPel)
Centro de Desenvolvimento Tecnológico (CDTEC)
Programa de Pó-Graduação em Computação (PPGC)
Rua Gomes Carneiro, 1 - 96010-610-Pelotas-RS-Brazil
Email: {joao.marins, tmcabreira, paulo}@inf.ufpel.edu.br

***Abstract*—An energy model for a quadcopter based on the dynamic of the movement and on the Physics principles of superposition and energy conservation is proposed here. Its accuracy was checked against another model published recently in the literature, which is based on experiments carried on specifically for that purpose. The model fits the experimental data and can be easily extended for other types of multi-rotors because is a function of quadcopter parameters. More than that, as it is based only on the dynamic of the movement equations, it is differentiable and integrable, and can be applied even to gasoline-powered drone, provide that we know the efficiencies of the combustion motors. It was also studied which simplifications are allowed without compromising its accuracy, for instance, drag effects. The model confirms that there is an optimal velocity for different flight path lengths and allows to calculate that velocity. Finally, the model was used to calculate the energy consumption during a real flight with a good result and it was also applied to obtain accurate results related to energy consumption during turning maneuvers.**

## I. Introduction

Unmanned Aerial Vehicles (UAVs) have taken a special role in recent years. Remotely controlled or flying autonomously, UAVs are a good option for applications that can be harmful to people or that are located in hostile environments. Among them, ice management information gathering [1], land mines detection [2] and power lines inspection [3]. Gradually, other non hazardous tasks are added to those above such as surveillance, delivery [4] or following events [5].

Usually, UAVs are classified into fixed-wing and rotor types. The second ones are extremely versatile. They can take-off and land vertically and hover over a fixed point. Among them, the quadrotor (or quadcopter) is the most popular due to the easy construction and control [6].

The two main limitations when using a UAV are the payload it can carry and its autonomy. The second depends on the weight, what includes the payload and the battery [4]. When a UAV is sent to perform a task, it is desirable that it completes the task and returns safely to a previously determined point. In this case, it would be very useful if we could estimate the amount of energy necessary to do that. Furthermore, researchers have been considered energy consumption as a metric in optimization criteria in coverage path planning missions [7]–[10]. However, all the works found so far define power as a function either of voltage-current or of propellers rotation. Those approaches do not consider the characteristics of the UAV and, thus, are not generic ones.

This paper proposes an energy model for a quadcopter based on Physics principles of the dynamic of the movement. The model can be extended for other types of multi-rotor UAVs, since it only depends on Physics parameters (gravity, air density) and vehicle parameters (mass, propeller size, etc.). The main contribution here is a closed-form energy model that has been validated with success against published data.

A closed-form is always useful because it can be easily differentiated or integrated, what allows the use in state-space model for energy. The main goal is to estimate the UAV energy consumption during the planning phase, during flight or to compare different paths. The same model allowed us to confirm the affirmative from [10] that there is an optimal velocity that leads to minimal energy consumption. Those values can be easily calculated and were the same obtained in that reference. Besides that, the paper demonstrates that the model can be used to compare two different paths in terms of energy consumption.

The remainder of this paper is organized as follows: in Section II we review the work we found on energy models. Section III describes the proposed energy model for a quadcopter. Section IV validates the model against experimental data. Section V presents an example of application for the proposed model. Conclusions are provided in Section VI.

## II. Related Work

In [11], authors discuss the effects of having more than four rotors on a micro aerial vehicle (MAV). They calculate the power to get a certain thrust from a rotor and use that information to model several types of multi-rotor to compare their dynamics, efficiency and redundancy. They do not analyze the movement along a flight path. [4] derives the power consumed by a multi-rotor drone in hover, but not during flight, take-off, or landing. The main focus is to relate the consumed power to the UAV weight.

An affirmation in [12] states that “It is not an easy task to derive a formal equation for the energy spent during a mission and if such an equation exists, it would be nonlinear and not easy to deal with”. As [11], they state that the consumed energy is proportional to the generated thrust and use that

relation to execute minimal-energy planning for a quadcopter based on the flight time. They do not consider any maneuver and do not obtain a closed-form equation.

Electric equations from the DC brushless motors, in which the rotations are included, are used by [13] to model the energy of a quadcopter. The result is a state equation model with 16 states. They calculate the energy for a previous defined path and also find a path corresponding to fixed energy, in a simulated environment using Matlab®.

In [14], the flight path is divided in three phases as in the model proposed here. As they focus on long paths, they disregard the first and the last parts of the path. The energy is related to the propeller rotation $\omega$. For a nonlinear model of the system, it uses model predictive controller (MPC) to determine the desired control inputs for each possible goal and the respective energy it needs for each goal. Wind disturbances are included in the state-space model as a force proportional to the wind velocity.

An energy model is proposed in [10], where the power is established from electric equations. The authors analyze a generic UAV flight during hovering, climbing, descending, accelerating, decelerating, flying at constant speed, and rotating. They present real flight results and the curves obtained show that there is an optimal velocity for each straight path length. The authors suggest splitting the whole path in several shorter paths of distance $d$. Flying those paths at the optimal velocity would lead to the lowest energy strategy. The energy is calculated using a look-up-table from data measured during the flight. That characteristic make the model be specific for the one used in the experiments.

## III. Proposed Model

A model is defined in [15] as a simplified representation of the essential aspects of an existing system (or a system to be constructed), which presents the knowledge of the system in a usable form.

Equations or sets of equations describing a model are an approximation of the real world. That means it is impossible to incorporate all characteristics of the process or system to be studied. There will be always a trade-off between the cost to reach the final model (time and effort to obtain and verify the model) and the level of details the model includes.

The model proposed here is based on the superposition principle and it was generated using only energy equations from Physics. It considers that the energy the drone needs to fly over a straight line with constant speed is the sum of the energy needed to keep the drone hovering plus the energy needed to overcome the air resistance. If the drone accelerates from zero to an specific velocity, the energy needed to increase the kinetic energy must be considered.

In the same way, when the drone performs a complete circular curve of radius $r$ with constant speed in a time $t$, the total energy is the sum of the energies to keep hovering during $t$ plus the energy needed to rotate the drone 360 degrees. The energy to hover is the power to hover multiplied by the time it hovers. The following subsections describe the Physics used to obtain the mathematical model.

### A. Power to Hover

When the drone hovers at a constant altitude, the velocity and the acceleration are zero. The zero acceleration means that the sum of the forces acting on it is zero. The propellers together, each one driven by a brushless DC motor, exert a force that equals the drone weight.

In order to calculate the electric power supplied by the battery to keep the drone hovering ($P_{hov}$), the efficiency of the electric motors ($\eta_{mot}$) as well as those of the propellers ($\eta_{prop}$) should be taken into account.

Let $P_0$ be the total power furnished as output of the electric motors. Then, $P_{hov}$ is

$$P_{hov} = \frac{P_0}{\eta_{mot} \times \eta_{prop}} = \frac{P_0}{\eta_{tot}} \tag{1}$$

$P_0$ can be determined by the concept of linear momentum [16]. From Figure 1, the air at point 1 (zero velocity) is forced to a velocity $v_2$ at point 2. $v_3 \approx v_4$ and it can be demonstrated that

$$v_3 = \frac{v_1 + v_2}{2}$$

So,

$$F_s = \dot{m} \times (v_2 - v_1) = \rho_{air} \times A \times v_3 \times (v_2 - v_1) =$$

$$= \rho_{air} \times A \times \left(\frac{v_1 + v_2}{2}\right) \times (v_2 - v_1)$$

$$F_s = \rho_{air} \times A \times \frac{(v_2)^2}{2} \tag{2}$$

where $F_s$ is the force propellers apply to the mass of air, $\dot{m}$ is the mass of air that is forced down by the propellers per second, $\rho_{air}$ is the value of the air density normally used, $A$ is the area (close to the propeller) the mass of the air pass through, $g$ is the gravitational constant, $v_2$ and $v_1$ are the velocities of the mass of the air in two different points.

This force equals the drone weight.

$$F_s = \rho_{air} \times A \times \frac{(v_2)^2}{2} = m \times g$$

$$v_2 = \left(\frac{2 \times m \times g}{\rho \times A}\right)^{(\frac{1}{2})} \tag{3}$$

As $P = F \times v$,

$$P_0 = \frac{\rho \times A \times {v_2}^3}{2} = \left(\frac{2}{\rho \times A}\right)^{\frac{1}{2}} \times (m \times g)^{\frac{3}{2}} \tag{4}$$

and

$$P_{hov} = \frac{\left(\frac{2}{\rho \times A}\right)^{\frac{1}{2}} \times (m \times g)^{\frac{3}{2}}}{\eta_{tot}} \tag{5}$$

Equation 5 shows that the power to keep the drone hovering is a function of the mass of the drone, area of the propeller, air density and gravity. Both motor and propeller efficiencies affects the final value as well.

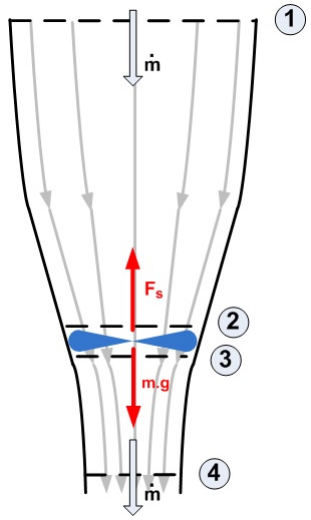


Fig. 1: Determining power to hover.

### B. Energy Model for a Horizontal Flight

Now, assume a drone flying a straight path of $d$ meters, as illustrated by Figure 2. At $t_0$, it starts with $v_0$. It accelerates until reaches velocity $v$ at $t_1$. It keeps the velocity until $t_2$ and it decelerates to $v_0$ at $t_3$.

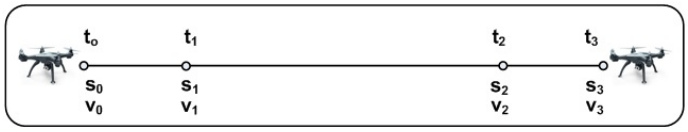


Fig. 2: Scenario for a straight line flight.

During the first and the last part, a force is needed to accelerate and decelerate the drone. The energy consumed for those parts can be calculated using the Energy Conservation Theorem as below.

**Phase 1:**

$$(v_1)^2 = (v_0)^2 + 2 \times a \times (s_1 - s_0)$$

$$(s_1 - s_0) = \frac{(v_1)^2}{(2 \times a)}$$

$$(t_1 - t_0) = \frac{v_1}{a}$$

**Phase 3:**

$$(v_3)^2 = (v_2)^2 - 2 \times a \times (s_3 - s_2)$$

$$(s_3 - s_2) = \frac{(v_2)^2}{2 \times a}$$

$$(t_3 - t_2) = \frac{v_2}{a}$$

However, in the second part of the path ($s_1$ to $s_2$) there is no acceleration and, therefore, no forces acting on the drone. The only energy consumed is to keep its altitude ($P_0 \times (t_2 - t_1)$).

**Phase 2:**

$$(s_2 - s_1) = d - (s_3 - s_2) - (s_1 - s_0) =$$

$$= d - \frac{(v_2)^2}{2 \times a} - \frac{(v_1)^2}{2 \times a}$$

$$(t_2 - t_1) = \frac{(s_2 - s_1)}{v_1} = \frac{d - \frac{(v_2)^2}{2 \times a} - \frac{(v_1)^2}{2 \times a}}{2 \times a} =$$

$$= \frac{d}{v_1} - \frac{(v_2)^2}{2 \times a \times v_1} - \frac{(v_1)^2}{2 \times a \times v_1}$$

The energy consumption during the whole path is:

$$E = (t_3 - t_0) \times P_0 + \frac{1}{2} \times m \times (v_1)^2 + \frac{1}{2} \times m \times (v_1)^2$$

$$E = [(t_1 - t_0) + (t_2 - t_1) + (t_3 - t_2)] \times P_0 + m \times (v_1)^2$$

$$E = \left[\frac{v_1}{a} + \frac{d}{v_1} - \frac{(v_2)^2 + (v_1)^2}{2 \times a \times v_1} + \frac{v_2}{a}\right] \times P_0 + m \times (v_1)^2 \quad (6)$$

The first term is the energy the drone needs to keep itself at the same altitude (hover) during the path flight ($s_0$ to $s_3$). The second and third terms represent the consumed energy to accelerate and decelerate the drone ($s_0$ to $s_1$ and $s_2$ to $s_3$).

Now, assume that the velocities $v_1$ and $v_2$ are the same, and call it $v$. During the first part of the path it accelerates from 0 $m/s$ to $v$ $m/s$. Then, it flies at $v$ $m/s$ for $(t_2 - t_1)$ seconds and it decelerates from $v$ $m/s$ to 0 $m/s$. Thus, the final equation can be simplified as below

$$E = \frac{1}{\eta_{tot}} \times \left[\left(\frac{d}{v} + \frac{v}{a}\right) \times P_0 + m \times v^2\right] \quad (7)$$

where $d$ is the total path length, $a$ is the maximum acceleration/deceleration, $m$ is the mass of the drone and $v$ is the velocity the drone flies most of the path.

Note that the energy necessary to overcome the drag force is disregarded so far.

### C. Including Drag Force

The drag force is added based on the Physics principle of "*work of a force*". During the flight, the point of application of the drag force on the drone moves along the trajectory. The amount of work done to do that measure the energy necessary to keep the trajectory. The drag force can be written as [16]:

$$F_D = \frac{\rho}{2} \times C_D \times A_{eff} \times v^2 \quad (8)$$

where $\rho$ is the air density, $C_D$ is the drag coefficient and $A_{eff}$ is the effective area of the drone subject to the effect of the air resistance.

The effect of the drag force is included in the model that now becomes

$$E = \frac{1}{\eta_{tot}} \times \left[\left(\frac{d}{v} + \frac{v}{a}\right) \times P_0 + m \times v^2 + \right.$$

$$\left. + d \times \frac{\rho}{2} \times C_D \times A_{eff} \times v^2\right] \quad (9)$$

### D. Optimal Velocity

Inspecting Equation (9), it seems that there is an optimal velocity, with minimum energy consumption, for each path length. Those values can be determined simply by finding the partial derivative of the energy model with respect to the velocity and by equaling to zero.

$$\frac{\partial E}{\partial v} = (2\times m + d\times\rho\times C_D\times A)\times v^3 + \left(\frac{P_0}{a}\right)\times v^2 + (-d\times P_0) = 0 \tag{10}$$

Consider ($a = 1\ m/s^2$), constant. That equation has two imaginary roots and one real root which is the value of the optimal velocity. Clearly, it depends on the distance $d$.

Figure 3 presents the optimal velocity calculated for several distances and three models: the complete model, one without kinetic contribution and one without the drag contribution.

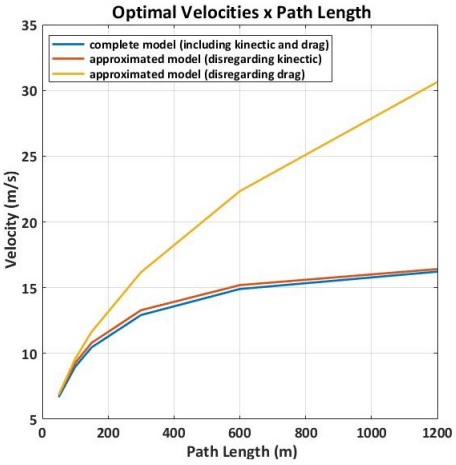


Fig. 3: Optimal velocity as a function of path length.

Two conclusions can be drawn from Figure 3. The first is that, for long paths, the optimal velocity tends to a limit. It is the same conclusion we found in [10], even though the values are not the same, probably due to differences on the parameters used for the two models.

The second conclusion is that the kinetic term can be left out. On the other hand, disregarding the drag term can lead to significant errors in optimal velocity calculation. Equation (11) makes clear each term considered or not in Figure 3.

$$E = \frac{1}{\eta_{tot}} \times \left[ \overbrace{\left(\frac{d}{v} + \frac{v}{a}\right) \times P_0}^{hover} + \overbrace{m \times v^2}^{kinetic} + \right.$$
$$\left. + \overbrace{d \times \frac{\rho}{2} \times C_D \times A_{eff} \times v^2}^{drag} \right] \tag{11}$$

## IV. Validation

The goal of this section is to validate the above mentioned model, by comparison with the graphics obtained in [10]. The parameters for the equations are those from the IRIS quadcopter, which are: $m = 1.3\ kg$ and $A = 0.2027\ m^2$ (four times the area of one $10'$ x $4.7'$ propeller). For gravity and air density, we used $g = 9.81\ m/sec^2$ and $\rho = 1.2928\ kg/m^3$. The value calculated by Equation 4 is $P_0 = 125.6\ Watts$.

### A. Power to Hover

The IRIS drone utilizes 4 brushless DC motors AC 2830, 850 kV. A study from the Army Research Laboratory [17] suggests a profile for the efficiency of very small brushed and brushless DC motors (weight less than 20 g). Even that the AC 2830, which weights 62 g, is out of the range of the study, we can use the equation on the right top of Figure 4 from [17] to have an idea of the value for the efficiency

$$\eta_{mot} = -64.84 \times 62^{-0.4317} + 95.66 = 84.7\%$$

Literature mentions the range for that efficiency between 70% and 100%. So, we are going to use the value of 90% for the motor efficiency ($\eta_{mot}$).

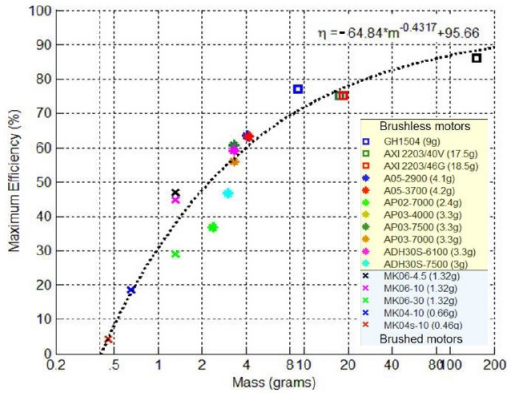


Fig. 4: Efficiency of a brushless motor from [17].

For the propeller efficiency ($\eta_{prop}$), the IRIS drone utilizes 4 Slow Flyer Propellers (2 SF + 2 SFP) with $10' \times 4.7'$ and pointy nose.

Wind tunnel measurements for nearly 140 propellers used on small UAVs and model aircraft are presented in [18]. It gives the efficiency value for different advance ratios $J$ which is defined as the ratio between the distance the propeller moves forward when it performs a complete rotation ($360^0$) and the blade diameter [19]. So, for a $10'$x$4.7'$ propeller, $J = 0.47$.

It can be used the classical formula

$$J = \frac{V}{n \times D}$$

where $V = v_2 = 10.24\ m/s$, calculated by Equation (3) and $n = 5,660\ rpm$ (60% of maximum rotation to keep hovering). The maximum rotation for a $850kV$ motor powered by a $11.1\ Volts$ battery package is calculated as $n_{max} = (850)\times(11.1) = 9,435\ rpm$. That leads to $J = 0.43$. From Figure 5, the propeller efficiency ($\eta_{prop}$) is around 65%. Thus, the power required from the battery to hover can be

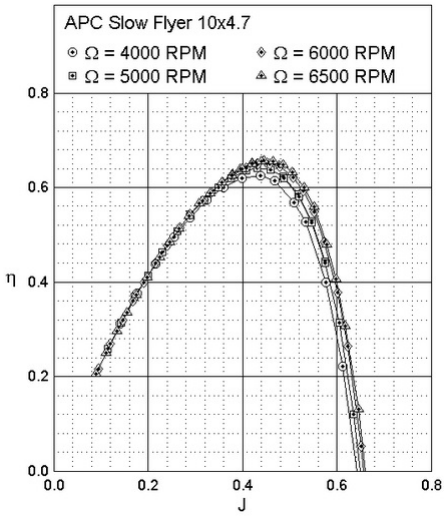


Fig. 5: Efficiency of the propeller from [18].

calculated as

$$P_{hov} = \frac{125.6}{(0.90) \times (0.65)} = 214.7\ Watts$$

This value is almost the same obtained experimentally in [10], 225 $Watts$.

### B. Horizontal Flight

In order to check if the model fits the reality, it was simulated to reproduce the curves obtained in [10]. The simulation used Equation 7 with parameters $m = 1.3\ kg$ and $a = 1\ m/s$, for distances 50, 100, 150, 300, 600 and 1,200 meters. The velocity varied from 1 $m/s$ to 14 $m/s$. The hover power ($P_{hov}$) considered was 214.7 $Watts$. Figure 6 shows the results, compared to the curves obtained from the model in [10].

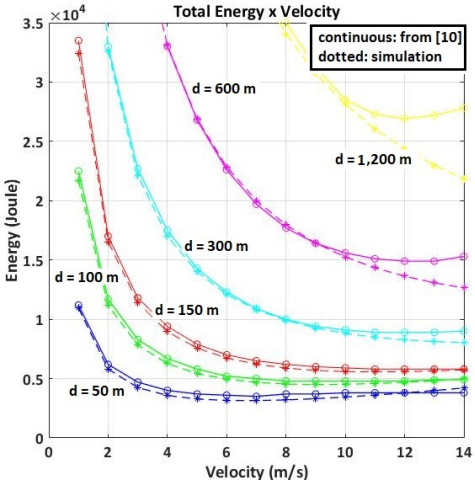


Fig. 6: Checking the energy model.

It can be noticed that, for velocities above 10 $m/s$, the proposed model indicates lower energy values than those obtained in [10]. That discrepancy is treated in the next topic.

### C. Including Drag Force

The model was checked again, now including the drag force, as can be seen in Equation 9. The parameters for the drag force are $\rho = 1.2928\ kg/m^3$ and $C_D \times A_{effect} = 0.01547\ m^2$. Figure 7 shows the results, again comparing the curves from simulation to those from [10].

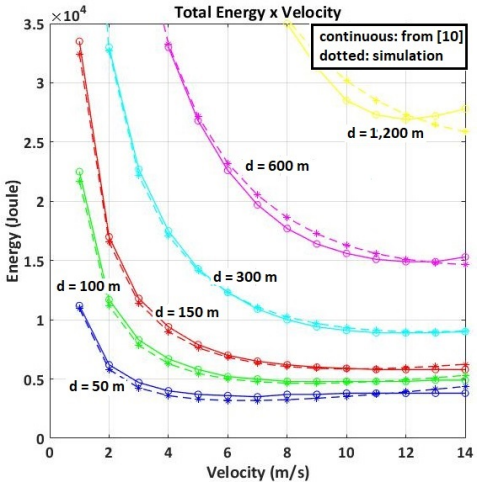


Fig. 7: Including the drag force.

Table I presents the differences between the values calculated using the model and the ones from [10].

TABLE I: Differences in Energy: Model × Curves from [10]

| $v\ (m/s)$ | $50\ m$ | $100\ m$ | $150\ m$ | $300\ m$ | $600\ m$ | $1,200\ m$ |
|---|---|---|---|---|---|---|
| 2 | $-6.3\%$ | $-4.4\%$ | $-2.6\%$ | $-1.0\%$ | $--$ | $--$ |
| 4 | $-10.2\%$ | $-6.1\%$ | $-4.4\%$ | $-2.4\%$ | $0.8\%$ | $--$ |
| 6 | $-11.4\%$ | $-3.7\%$ | $-2.4\%$ | $-0.1\%$ | $2.7\%$ | $--$ |
| 7 | $-8.9\%$ | $-4.7\%$ | $-2.5\%$ | $1.5\%$ | $4.1\%$ | $--$ |
| 8 | $-12.0\%$ | $-3.1\%$ | $-2.4\%$ | $2.4\%$ | $5.2\%$ | $1.1\%$ |
| 9 | $-8.8\%$ | $-3.4\%$ | $-1.7\%$ | $3.0\%$ | $5.2\%$ | $3.5\%$ |
| 10 | $-7.1\%$ | $-2.4\%$ | $-0.9\%$ | $2.4\%$ | $4.3\%$ | $5.9\%$ |
| 11 | $-2.4\%$ | $-0.2\%$ | $1.2\%$ | $2.3\%$ | $3.2\%$ | $4.5\%$ |
| 12 | $3.0\%$ | $2.7\%$ | $2.6\%$ | $1.2\%$ | $1.4\%$ | $1.6\%$ |
| 13 | $8.9\%$ | $4.2\%$ | $4.8\%$ | $1.0\%$ | $-0.6\%$ | $-2.8\%$ |
| 14 | $15.1\%$ | $8.4\%$ | $7.7\%$ | $0.5\%$ | $-4.2\%$ | $-7.0\%$ |

Adding the drag effect changed the shape of the curves for velocities above 10 m/s, reducing the discrepancies. However, despite the good approximation, the two curves are still not matching exactly, what can be due to several factors.

First, the value we are using for $P_{hov}$. Our proposed model assumes that the hover condition is that in which the drone has zero vertical velocity and zero vertical acceleration. The unique energy the drone consumes is that necessary to compensate the gravity. Theoretically, if the drone is hovering in an environment without any disturbances, that power should be constant.

In [10], that value is obtained experimentally with the drone hovering and we can see clearly that is almost impossible to keep the drone standing at a constant altitude. That fact can be seen if we analyze the log of a real flight. We did that with the spiral coverage on a rectangular area from [20]. The

whole flight took 298 seconds. Points with velocity close to zero (less than 0.02 m/s) were extracted from the log along with the acceleration (discounting gravity). For each point, the consumed power from the battery was calculated. Note that sometimes, even when vertical velocity is zero, due to the high vertical acceleration the drone requires a huge power from the battery. That happens for $t = 87\ s$. It reaches $253.2\ Watts$.

TABLE II: Analysis of Hover Situation

| Time (s) | Velocity $(m/s)$ | Accelaration $(m/s^2)$ | Power $(W)$ |
|---|---|---|---|
| 26 | $-0.01$ | 0.724 | 225.1 |
| 75 | 0.01 | 0.586 | 252.7 |
| 87 | 0.00 | $-1.182$ | 253.2 |
| 91 | 0.01 | 0.427 | 239.5 |
| 93 | $-0.01$ | 1.664 | 207.6 |
| 103 | 0.01 | $-0.194$ | 218.6 |
| 113 | $-0.01$ | 0.758 | 190.3 |
| 178 | 0.01 | 0.318 | 186.7 |
| 185 | 0.00 | 0.474 | 217.2 |
| 240 | 0.00 | 0.573 | 181.4 |

$P_{hov}$ is the most important component of the drone consumed power. For the same flight, and using the proposed model, we can separate each component, as shown in Figure 8. From that picture, we also understand the existence of an optimal velocity discussed in Subsection III-D. In order to minimize the energy consumption, the drone needs to increase velocity so that the time flying be reduced. However, when the velocity becomes higher, the drag effect increases either. The solution for this trade off is the optimal velocity and it depends on the flight distance.

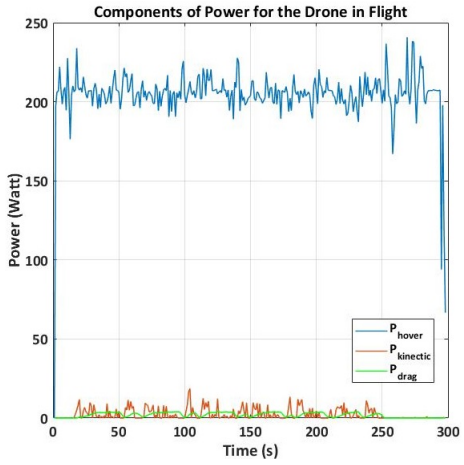


Fig. 8: Power components in a real flight.

Another factor is the accuracy of the parameters used for the model. Efficiencies, mass, drag coefficient and effective area were estimated or obtained from references, but need to be defined with more precision.

Finally, that difference could be also related to external factors like wind effects as well as to internal factors like sensor biases, sensor noises or errors integration.

## V. Applications

A model is extremely useful to come to conclusions without going to field tests, which can be expensive and risky. As we saw along this paper, the proposed model presents good adherence to the reality.

However, before using it in a practical way to compare two strategies, as we do in Section V-B, we will apply the model to estimate the consumed energy for a trajectory.

### A. Energy Consumption Estimation

We choose the spiral coverage over a rectangular area presented in [20] and depicted in Figure 9. In that paper, the authors used their model to estimate the energy and took a real flight to confirm the accuracy. We did the same with our proposed model.

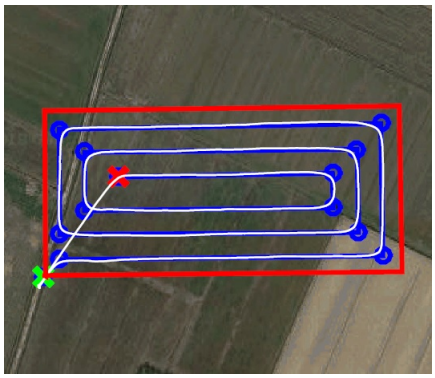

Fig. 9: Spiral coverage over a rectangular area from [20]

The path was divided in $45$ small parts (straights and curves) For each straight part of the coverage it was considered the acceleration, the constant velocity flight and the deceleration. We use the same velocity $(8.0\ m/s)$ for long parts and the reduction of $45\%$ in velocity before turns (called entrance speed in [20]). Acceleration was considered $1.0\ m/s^2$. We assumed that curves were made with constant entrance velocity $(4.4\ m/s)$. Table V shows the contribution of each component of the proposed model. The total energy value is $46,603\ Joules$, which is close to the value estimated by [20] $(46,681\ Joules)$ and below of the real value given in the same reference $(47,329\ Joules)$.

TABLE III: Model Applied to a Spiral Coverage

| Coverage Part | Status | $P_{hov}$ | $P_{kin}$ | $P_{drag}$ |
|---|---|---|---|---|
| straight paths | acceleration | 8,560 | 506 | 131 |
| straight paths | constant velocity | 27,286 | 0 | 1,096 |
| straight paths | deceleration | 6,848 | 434 | 128 |
| curves | constant velocity | 1,601 | 0 | 13 |
| | Total by component | 44,295 | 940 | 1,368 |

The differences between the value calculated by our model and the real value can be easily explained if we plot the velocity and the acceleration during the whole flight. Figure 10 shows the plot.

Two points call our attention. First, the drone does not always reach the velocity of 8 m/s. For some very short paths,

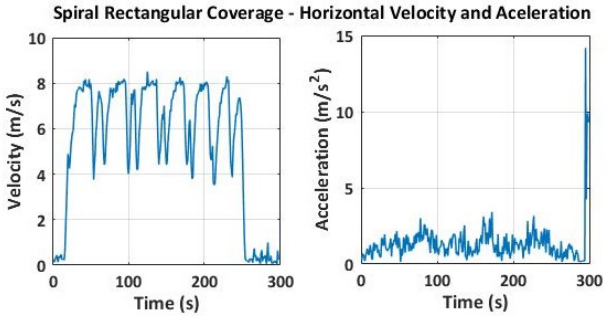


Fig. 10: Velocity and acceleration profiles for a real flight

it flies below 7 m/s. And when it turns, most of the times it does that at 4 m/s or less. Regarding the acceleration, the mean value during the whole coverage is 1.2 m/s$^2$, instead of 1.02 m/s$^2$ we used in the model.

As a final check, we adjusted those two values (velocity and acceleration) and calculated the energy again. Table IV shows the final result. The value calculated for energy consumption is 47,556 Joules, which is still close to the value estimated in reference (46,681 Joules), but almost the same indicated as the real value (47,329 Joules). The difference is less than 0.5%.

TABLE IV: Model Applied to a Spiral Coverage (Corrected)

| Coverage Part | Status | $P_{hov}$ | $P_{kin}$ | $P_{drag}$ |
|---|---|---|---|---|
| straight paths | acceleration | 7,472 | 499 | 97 |
| straight paths | constant velocity | 29,902 | 0 | 1,122 |
| straight paths | deceleration | 6,313 | 445 | 96 |
| curves | constant velocity | 1,601 | 0 | 9 |
| | Total by component | 45,288 | 944 | 1,324 |

### *B. Strategy Comparison*

As another application, the model above was used to test the strategy mentioned in [21] to make a 90-degree turn. Figure 11 illustrates the idea. It is worth mentioning in that reference the strategy was tested in a flight, but for a fixed-wing aircraft.

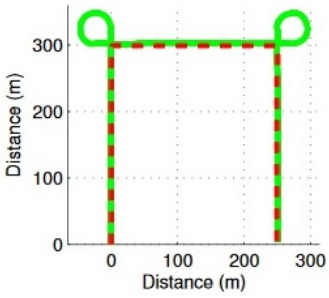


Fig. 11: Strategy to cover the path without missing points [21].

The question is "Considering the energy consumption, what is the best maneuver to avoid missing the square vertices? (1) Flying the straight lines with optimal velocity, reach the vertices with zero velocity and turn 90 degrees; or (2) Flying the whole path with the same optimal velocity avoiding the subtle 90-degree turn?"

The analysis presented here is more comprehensive since it is not limited to a right angle turn, as shown in Figure 12. The calculi presented here are for $\beta = 45^o$, but more values are in the end of this Section.

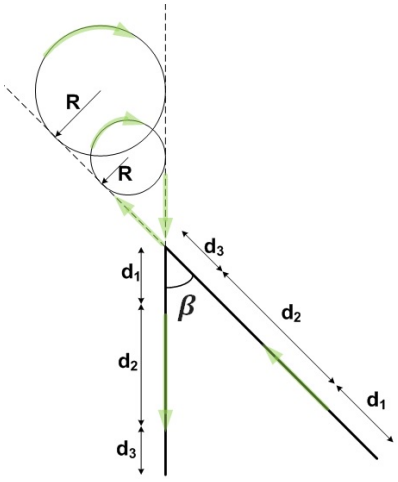


Fig. 12: Geometry involved in two strategies.

**Strategy 1:** For Strategy 1, the drone accelerates from zero velocity in $d_1$, keeps the optimal velocity in $d_2$ and decelerates to zero velocity in $d_3$. Then, it rotates an angle $(180^o - \beta)$ and repeats the procedure for the second branch. For this first analysis, $(d_1 + d_2 + d_3)$ was assumed as a 600-meter path, which has an optimal velocity, calculated by Equation 10 of 14.9 m/s. Total energy can be calculated as

$$E^1_{total} = E_{d1,d2,d3} + E_{turn} + E_{d1,d2,d3} \tag{12}$$

The first and last term are calculated using Equation 9. The middle term depends on the time drone takes to turn the angle and is calculated as

$$E_{turn} = \frac{\left(\pi - \frac{\beta \times \pi}{180^o}\right)}{\omega_{max}} \times P_{turn} \tag{13}$$

Note that, in order to make a quadcopter turn, two opposite motors need to have their rotations reduced. But to stay at the same altitude the thrust forces must be kept. So, the other two motors increase their rotation. It means the turning power is the same power to keep hovering, except that, in this situation, the rotations are unbalanced. Then,

$$E_{turn} = \frac{\left(\pi - \frac{\beta \times \pi}{180^o}\right)}{\omega_{max}} \times P_{hov} \tag{14}$$

For $\beta = 45^o$,

$$E^1_{total} = 15,043 + 265 + 15,043 = 30,351\ Joules.$$

**Strategy 2:** For Strategy 2, the drone keeps the optimal velocity during the whole path, turning $(180^o + \beta)$ degrees. Note that the second path is longer than the first one. The difference between them is

$$L_2 - L_1 = 2 \times R \times \left(\frac{1 + cos(\beta)}{sin(\beta)}\right) + R \times \left(\pi + \frac{\beta \times \pi}{180^o}\right) \tag{15}$$

where $R = \frac{v_{opt}}{\omega_{max}}$ and depends on the maximum turning rate of the drone. For this case, from [10], $\omega_{max} = 2.1\ rad/s$.

Also note that, in this case, $L_2$ depends on $R$ which depends on $v_{opt}$, calculated as function of $L_2$, which is the variable $d$ in Equation 10. Without loss of precision, we are going to approximate $L_2$ by $2 \times (d_1 + d_2 + d_3)$, disregarding the curve. Then, for $L_2 \approx 1,200\ meters$. For that length, the optimal velocity is $16.2\ m/s$, $R = 7.7\ m$ and $L_2 = 1,258\ m$. So, the difference in length is less than $5\ \%$.

The drone flies the 1,258-meter path at the same constant velocity of $16.2\ m/s$ in about 78 seconds. It needs power to overcome the drag force. However, no extra power is needed to turn, except the power to hover as explained for Strategy 1. The total energy is calculated using Equation 9, but disregarding the terms related to acceleration and deceleration

$$E = \left(\frac{d}{v}\right) \times P_{hov} + (d) \times \frac{\rho}{2} \times C_D \times A_{eff} \times v^2 \qquad (16)$$

$$E^2_{total} = 18,337 + 6,750 = 25,087\ Joules$$

The results contradict what is said in [21]. However, we must take into account that their results are for a fixed-wing UAV. That craft has much less maneuverability than a quadcopter, mainly because their movement variables are coupled. Due to that, what was supposed to be a circle is transformed into a very big ellipse, which has almost the same length of the path.

The calculus can be extended to other $d$ and $\beta$ as showed in Table V. The values represent the percentage of energy reduction when Strategy 2 is applied.

TABLE V: Energy Reduction for Strategy 2

| $d_1 + d_2 + d_3$ | $\beta = 30^o$ | $\beta = 45^o$ | $\beta = 60^o$ | $\beta = 90^o$ |
|---|---|---|---|---|
| 300 meters | 33.6 % | 28.7 % | 31.4 % | 29.6 % |
| 600 meters | 20.6 % | 17.3 % | 19.1 % | 17.9 % |
| 1,200 meters | 11.1 % | 9.2 % | 10.2 % | 9.5 % |

## VI. Conclusion

In this paper, we proposed an energy model for a quadcopter in a closed-form based on the dynamic of the movement and on the Physics principles of superposition and energy conservation. The model was validated using experimental data published very recently. The model allows us to confirm the hypothesis that there is an optimal velocity, in terms of energy consumption, for each path length. Those velocities were calculated and matched the values determined in the experiments. The proposed model can be extended easily to different types of multi-rotors UAVs, by changing the parameters. Besides that, it is differentiable and integrable and can be used for gasoline powered drones.

The model was used in two applications. First, it calculated the energy consumption of an specific trajectory and had the result matching those from a real flight. Second, two different strategies to make a curve during flight were compared for three different path lengths and four different turning angles.

In the near future, the use of probabilistic filters incorporating this model will allow us to estimate more precisely and continuously the energy needed to perform tasks like package delivery or area coverage.

## References


[1] A. Stalmakou, "Uav/uas path planning for ice management information gathering," Master's thesis, Norway, 2011.

[2] C. Castiblanco, J. Rodriguez, I. Mondragon, C. Parra, and J. Colorado, *Air Drones for Explosive Landmines Detection*. Springer International Publishing, 2014, pp. 107–114.

[3] C. Liu, Y. Liu, H. Wu, and R. Dong, "A safe flight approach of the uav in the electrical line inspection," *International Journal of Emerging Electric Power Systems*, vol. 16, no. 5, pp. 503–515, 2015.

[4] K. Dorling, J. Heinrichs, G. G. Messier, and S. Magierowski, "Vehicle routing problems for drone delivery," *IEEE Transactions on Systems, Man, and Cybernetics: Systems*, vol. 47, no. 1, pp. 70–85, 2017.

[5] D. Zorbas, T. Razafindralambo, F. Guerriero *et al.*, "Energy efficient mobile target tracking using flying drones," *Procedia Computer Science*, vol. 19, pp. 80–87, 2013.

[6] M. K. N. Shah, M. B. J. Dutt, and H. Modh, "Quadrotor–an unmanned aerial vehicle," *International journal of Engineering development and research*, vol. 2, no. 1, pp. 1299–1303, 2014.

[7] D. Li, X. Wang, and T. Sun, "Energy-optimal coverage path planning on topographic map for environment survey with unmanned aerial vehicles," *Electronics Letters*, vol. 52, no. 9, pp. 699–701, 2016.

[8] O. Artemenko, O. J. Dominic, O. Andryeyev, and A. Mitschele-Thiel, "Energy-aware trajectory planning for the localization of mobile devices using an unmanned aerial vehicle," in *Computer Communication and Networks (ICCCN), 2016 25th International Conference on*. IEEE, 2016, pp. 1–9.

[9] C. Nattero, C. T. Recchiuto, A. Sgorbissa, and F. Wanderlingh, "Coverage algorithms for search and rescue with uav drones," in *Artificial Intelligence, Workshop of the XIII AI*IA Symposium on*, 12 2014.

[10] C. Di Franco and G. Buttazzo, "Coverage path planning for uavs photogrammetry with energy and resolution constraints," *Journal of Intelligent & Robotic Systems*, pp. 1–18, 2016.

[11] M. Achtelik, K.-M. Doth, D. Gurdan, and J. Stumpf, "Design of a multi rotor mav with regard to efficiency, dynamics and redundancy," in *AIAA Guidance, Navigation, and Control Conference*, 2012, p. 4779.

[12] A. Chamseddine, Y. Zhang, C. A. Rabbath, C. Join, and D. Theilliol, "Flatness-based trajectory planning/replanning for a quadrotor unmanned aerial vehicle," *IEEE Transactions on Aerospace and Electronic Systems*, vol. 48, no. 4, pp. 2832–2848, 2012.

[13] F. Morbidi, R. Cano, and D. Lara, "Minimum-energy path generation for a quadrotor uav," in *Robotics and Automation (ICRA), 2016 IEEE International Conference on*. IEEE, 2016, pp. 1492–1498.

[14] N. Bezzo, K. Mohta, C. Nowzari, I. Lee, V. Kumar, and G. Pappas, "Online planning for energy-efficient and disturbance-aware uav operations," in *Intelligent Robots and Systems (IROS), 2016 IEEE/RSJ International Conference on*. IEEE, 2016, pp. 5027–5033.

[15] E. Pieter, "System identification: parameter and state estimation," 1974.

[16] S. Yeong and S. Dol, "Aerodynamic optimization of micro aerial vehicle." *Journal of Applied Fluid Mechanics*, vol. 9, 2016.

[17] A. M. Harrington and C. Kroninger, "Characterization of small dc brushed and brushless motors," ARMY RESEARCH LAB ABERDEEN PROVING GROUND MD VEHICLE TECHNOLOGY DIRECTORATE, Tech. Rep., 2013.

[18] G. Ananda. Uiuc - propeller database volume 1.

[19] D. Wall, "Optimum propeller design for electric uavs," Ph.D. dissertation, 2012.

[20] T. Cabreira, P. Ferreira, C. Di Franco, and G. Buttazzo, "Energy-aware spiral coverage path planning for uav photogrammetric applications," *IEEE Robotics and Automation Letters*, vol. –, no. –, pp. –, 2018.

[21] A. Xu, C. Viriyasuthee, and I. Rekleitis, "Optimal complete terrain coverage using an unmanned aerial vehicle," in *Robotics and automation (ICRA), 2011 IEEE international conference on*. IEEE, 2011, pp. 2513–2519.